Real-time Identification of Behavior Leading to Capsize

Leigh McCue, *Aerospace and Ocean Engineering, Virginia Tech*

Christopher Bassler*, Aerospace and Ocean Engineering, Virginia Tech*

William Belknap, *Seakeeping Division, Naval Surface Warfare Center, Carderock Division*

ABSTRACT

In this paper the authors present a methodology to detect instabilities leading to capsize in real-time. Specifically, variations in finite-time Lyapunov exponent (FTLE) time series are identified from experimental data. As shown in prior work, FTLEs have potential, both numerically and experimentally, to indicate the onset of chaotic behavior leading to capsize through detection of idiosyncrasies in the FTLE time series. The principle objective of this work is to identify instabilities from experimental data without dependence upon time-consuming numerical simulation. A demonstration of the concept is given through application to experimental data for a notional destroyer model (DTMB model 5514).

Keywords: *capsize, chaos, finite-time Lyapunov exponent*

1. INTRODUCTION

Large amplitude vessel motions and capsize have served as hazards of the maritime community for centuries. Therefore, it is of benefit to all sectors of the marine industry to develop tools which could provide mariners with indicators of the onset of inclement ship motions. Establishing a tool to aid vessel operators in identifying the onset of threatening ship motion conditions would allow time for changes to be made, thus altering the commanded response to environmental conditions and possibly reducing exposure to devastating ship motions or capsize. For large amplitude ship motions and capsize, small variations in wave and/or position initial conditions can result in largely varying end behavior. Finite-time Lyapunov exponents (FTLEs) measure convergence or divergence of nearby trajectories thus providing a quantitative measure of a system's sensitivity to initial conditions and an indication of long-term behavior for a chaotic system. FTLEs are

feasible for use as a predictive tool to provide early warnings for vessel instabilities, or motions leading to capsize.

For a system of equations written in state-space form $\dot{\mathbf{x}} = \mathbf{u}(\mathbf{x})$, small deviations from the fiducial trajectory can be expressed by the equation $\delta\dot{x}_i = (\partial u_i / \partial x_j)\delta x_j$ (Eckhardt & Yao, 1993). $\delta\mathbf{x}$ is a vector representing the deviation from the trajectory with components for each state variable of the system. From this, the equation for the finite-time Lyapunov exponent can be written as Equation 1 (Eckhardt & Yao, 1993).

$$\lambda_T(\mathbf{x}(t),\delta\mathbf{x}(0)) = \frac{1}{T}\log\frac{\|\delta\mathbf{x}(t+T)\|}{\|\delta\mathbf{x}(t)\|} \qquad (1)$$

Positive FTLEs indicate exponential divergence of a nearby trajectories and conversely, negative FTLEs indicate exponential convergence. That is, if one were to envision an infinitesimal ball of points surrounding an initial point along the fiducial trajectory, FTLEs measure whether that ball stretches into an ellipsoid, contracts to a point,

or remains a ball over small increments in time. If any one principal axis of the ball grows at an exponential rate over a time increment, there will be a positive FTLE for this time increment. (Or, in the asymptotic sense, if as time approaches infinity one finds exponential growth, there is at least one positive Lyapunov exponent.)

Methods for computing Lyapunov exponents and FTLEs from equations of motion are well developed in references such as Benettin *et al.* (1980), Wolf *et al.* (1985), and Eckhardt & Yao (1993). In this work, FTLEs from experimental time series are calculated based on a modified version of the algorithm developed for Lyapunov exponents by Sano & Sawada (1985)[1]. While Lyapunov exponents have been used to demonstrate chaotic behavior for numerous naval architecture applications such as Papoulias (1987), Falzarano (1990), Spyrou (1996), Murashige and collaborators (1998a; 1998b; 2000), Arnold *et al.* (2003), McCue & Troesch (2004; 2005) and McCue, Belknap, & Campbell (2005), it is only recently that FTLEs have been exploited for the purposes of anticipating ship motions. See, for example, works by McCue & Bassler (2005), McCue (2005), McCue & Troesch (2006), and McCue & Bulian (2006).

A demonstration of the concept is given through application to experimental data for a notional destroyer model (DTMB model 5514). Over 100 experimental runs were conducted in regular waves to examine the capsize behavior of the $1/46.6^{th}$ scale model (full-scale ship length is 142.04 m). Run conditions were at nominal Froude numbers from 0.1 to 0.4, wave length to ship length (λ/L) of 0.75 to 1.5, wave height to wave length (H/λ) of 1/10 to 1/20, and ship headings ranging from following to stern-quartering to beam seas. The term 'nominal' is used with respect to Froude number because the propeller shafts are given a commanded voltage corresponding to an equivalent calm water speed, rather than prescribing speed specifically. Further discussion is provided in Section 2 on model test details. This paper focuses upon 37 capsize and non-capsize tests in stern-quartering seas, that is, 45 degrees off the stern, identified as a dangerous heading. FTLE methods are applied to model 5514 experimental data analyzed in a variety of wave conditions to illustrate the generality of the method.

2. MODEL TEST DETAILS

The model 5514 regular wave dynamic stability test was performed in the Maneuvering and Seakeeping Basin at the Carderock Division of the Naval Surface Warfare Center in November, 2004. Figure 1 shows model 5514 during a dynamic stability run in regular waves. The model was radio controlled, self-propelled, and free in all 6 degrees of freedom. A PID controller autopilot was used to maintain the desired heading, while the motor powering the two propeller shafts was given a constant voltage equal to the voltage needed to achieve the desired model speed in calm water. Because the model is self-propelled with an autopilot, forward speed and heading do oscillate with wave interaction over the course of an experimental run (McCue *et al.*, 2005). For the model runs analyzed in this study, the KG was set such that the calm water range of positive stability was approximately 70 degrees. Instruments measured roll, roll rate, pitch, pitch rate, heading, yaw rate, and ship-referenced accelerations at several points. The initial conditions of the simulation were not controlled, but rather the model was accelerated out of the corner of the basin into the wave field at essentially random points relative to the wave phase. The initial heading was nominally the desired heading.

---

[1] The Sano and Sawada algorithm is quite similar to that proposed by Eckmann *et al.* (1986).

Figure 1: DTMB Model 5514 in regular seas.

3. METHODOLOGY

As in prior Stability Workshop papers (McCue & Troesch, 2004; McCue *et al.*, 2005), the basis for the algorithm used to calculate Lyapunov exponents is that detailed in Sano & Sawada (1985). Tangent space methods for Lyapunov exponent calculations were developed simultaneously by the separate research teams of Sano & Sawada (1985) and Eckmann and coauthors (1985; 1986). This approach allows for calculation of the full spectrum of Lyapunov exponents through local predictions of the Jacobian along the time series trajectory. For example, for a given trajectory $\mathbf{x}(t)$ defined by Equation 2, the tangent vector ξ is given by the linearized form of Equation 2 presented in Equation 3 where $\mathbf{J}$ is the Jacobian matrix of $\mathbf{f}$, $\mathbf{J} = \partial \mathbf{f} / \partial \mathbf{x}$ (Sano & Sawada, 1985). Sano & Sawada (1985) solve Equation 3 through a least squares estimate of the time dependent linear operator A_j which approximates the map from $\xi(0)$ to $\xi(t)$.

The Lyapunov exponents are then computed using Equation 4 where τ is a flow scale time increment, n is the number of data points, and $\mathbf{e}$ is an orthonormal basis maintained using a Gram-Schmidt renormalization process (Sano & Sawada, 1985). For details of this process refer to Sano & Sawada (1985) or the similar works of Eckmann *et al.* (1985; 1986).

$$\dot{\mathbf{x}} = \mathbf{f}(\mathbf{x}) \qquad (2)$$

$$\dot{\xi} = \mathbf{J}(\mathbf{x}(t)) \cdot \xi \qquad (3)$$

$$\lambda_i = \lim_{n \to \infty} \frac{1}{n\tau} \sum_{j=1}^{n} \ln \left\| A_j e_i^j \right\| \qquad (4)$$

To overcome the difficulties associated with the brevity of the DTMB Model 5514 experimental data, time series for all runs conducted at the same target heading were treated as containing possible neighbors for all other time series at that heading. For the case of stern-quartering seas, rather than solely searching the single recorded time history of interest for neighboring points with which to approximate the Jacobian of the system, all model runs released in stern quartering seas were searched for neighboring points for each instant of interest in the analyzed time history. In order to demonstrate the generality of this method, all wave conditions were grouped for each given heading, that is to say, in searching for neighboring points it is deemed just as acceptable to search time series with differing wave heights and lengths and forward speeds because they yield as much information as to the ship's mechanism of response as those runs with identical wave conditions. In addition, this allows for added realism as typical seaways contain a spectrum of wave heights and frequencies and any method to detect instabilities must be capable of identifying stability trends in varying sea conditions.

Additionally, in this work, roll, pitch, roll rate, and pitch rate time series were used rather than embedding single variate roll time series data as done previously for Lyapunov exponent calculations (McCue *et al.*, 2005). Since multi-variate data was readily available, this approach was taken to potentially improve the accuracy of the algorithm and remove the limitations inherent in embedding. This approach restricts the dimensionality of the system to 4, and therefore it is possible that higher order information about the attractor is lost. However, it is hoped that with four variables, the primary attractor dynamics are captured. Increasing the dimensionality of the system would run the risk of spurious

exponents, increased computation times, and/or numerical inaccuracies. Only rotational state variables (and their associated derivatives) were chosen to avoid dimensionality concerns associated with mixing displacements and rotations.

Table 1 compares values for the first Lyapunov exponent calculated using the previous, more simplistic approach, embedding univariate roll time history data into 5 dimensions and using the individual time series data to calculate Lyapunov exponents (Method 1), to the modified approach detailed above (Method 2)[2]. For each analyzed run under Method 2, 37 separate time histories were scanned for 'neighbors' to each state space vector in time for the analyzed run.

For example, when calculating the Lyapunov exponent for Run 400, at each instant in time in Run 400, neighbors are selected from 36 additional time histories for the model in stern quartering seas, in addition to searching Run 400 for neighbors. As can be seen in Table 1 the agreement between the two methods is good given the time series length limit constraints.

Table 1: Table of largest Lyapunov exponents comparing model-scale results from embedded approach with d=5 (McCue *et al.*, 2005) to non-embedded approach. All cases non-capsize.

3	Experimental Data		Method 1, d=5	Method 2
Run #	*H/λ*	*λ/L*	*Lyap. Exp. (1/s)*	*Lyap. Exp. (1/s)*
400	0.0518	1.498	0.2066	0.2712
239	0.0679	0.998	0.2020	0.1929
313	0.0671	1.248	0.1270	0.3392
312	0.0681	1.246	0.7464	0.5146
418	0.0971	0.773	1.0724	0.6131
417	0.0999	0.750	0.7401	0.4293
281	0.1020	1.002	0.6341	0.4157
329	0.1003	1.252	0.6005	0.7922

---

[2] Note, all results in this paper are presented model scale. To reconcile the values given for Method 1 with those published in McCue, Belknap, and Campbell (2005), scale by $\sqrt{(L_M / L_S)} = 1/\sqrt{46.6}$.

4. FINITE-TIME LYAPUNOV EXPONENTS

Finite-time Lyapunov exponents are calculated using the same approach discussed previously for Lyapunov exponents in which all similar time series are treated as potential sources of neighbors for each analyzed run and time series consist of roll, pitch, roll rate and pitch rate data.

A simple flow chart detailing the steps in the computation of FTLEs is presented in Figure 2. Unlike the asymptotic Lyapunov exponent which is averaged over the entire length of the time series, finite-time Lyapunov exponents are calculated over short intervals of time, reference Equation 1. Algorithmically, anytime that insufficient neighbors were found with which to approximate the Jacobian of the system, the number -1000 was stored as a flag for the FTLE time series.
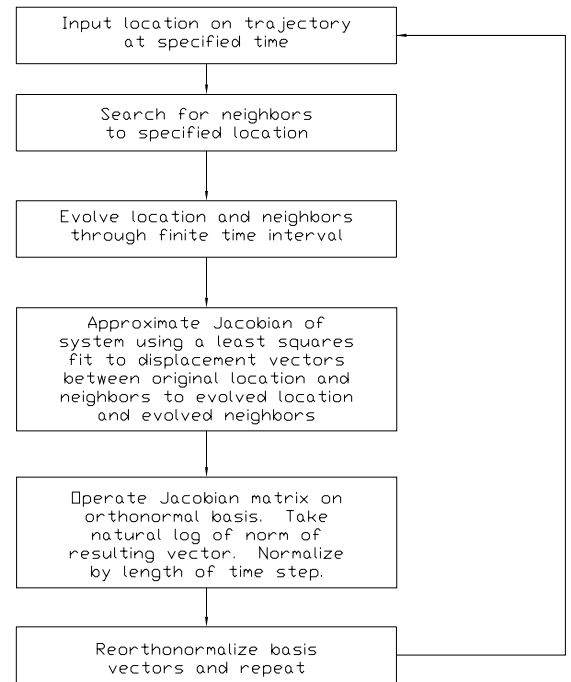
Figure 2: Flowchart for calculation of FTLEs.

Figures 3 and 4 show roll time histories, FTLE time histories, and roll/roll velocity phase space for similar capsize and non-capsize runs. In the capsize run, the point at which the trajectory leaves the stable attractor, as determined by examination of the phase

portrait, is marked with an 'x' on the phase space plot and vertical lines on the roll and FTLE time series.

For the non-capsize case run 329, large variations in the FTLE time series are observed at the onset and during large amplitude rolling. As apparent in the phase portrait, while roll conditions in excess of 70 degrees are encountered leading to complicated trajectories, capsize does not occur.

Conversely, Run 331 encounters much smaller roll motions until the oscillation immediately preceding that leading to capsize. In this case as well, large variations in the FTLE time series and/or the flag of a lack of appropriate neighbors is detected in advance of the trajectory's deviation from limit-cycle behavior.
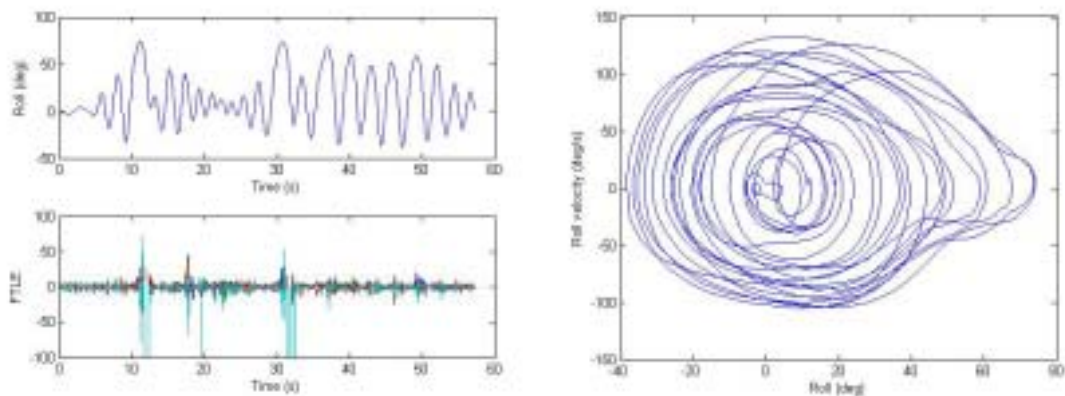

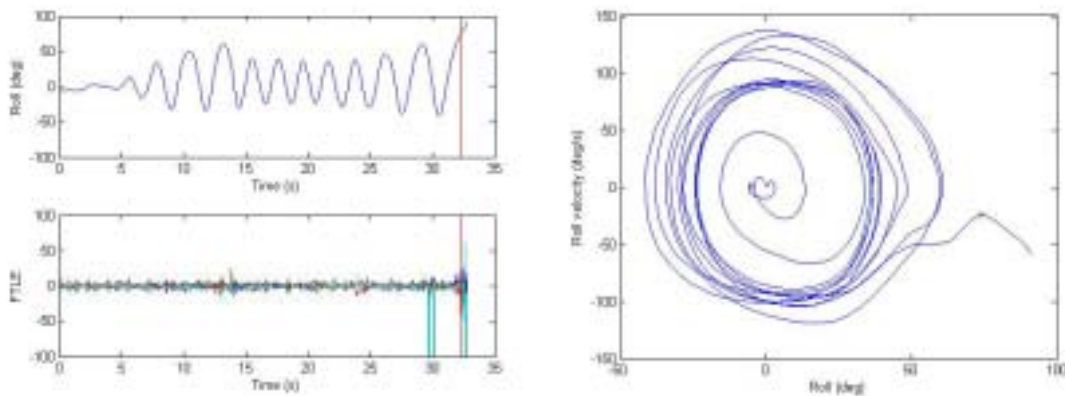Figure 3: No Capsize Run 329: H/λ=1/9.972, λ/L=1.252, Fn=0.40 released in stern quartering seas.

Figure 4: Capsize Run 331: H/λ=1/9.48, λ/L=1.228, Fn=0.40 released in stern quartering seas.

In an effort to tabulate quantifiable indicators of capsize. The FTLE time series for each run was scanned to identify if a critical value was exceeded, chosen as 20 1/s in order to be roughly twice the max FTLE$_1$ found in typical cases for these experiments, and/or if there were periods for which insufficient neighbors were found flagged in the FTLE

time series with the value -1000, *i.e.* behavior not regularly detected in any other time series. Those runs in which FTLE$_1$ exceeds the critical value and/or has periods with insufficient neighbors are then marked as potential dangers. Table 2 gives a summary of the analyzed runs including their run number, whether or not they were flagged for hazardous behavior, and whether or not the vessel ultimately capsized during that run.

Table 2: Summary of 37 DTMB hull 5514 experimental runs indicating capsize/non-capsize and if hazardous periods were identified using FTLE analysis.

Run#	H/λ	λ/L	Fn	Hazard	Capsized	Run#	H/λ	λ/L	Fn	Hazard	Capsized
212	0.092	0.748	0.20	No	No Capsize	312	0.068	1.246	0.40	Flag	No Capsize
213	0.091	0.750	0.20	No	No Capsize	313	0.067	1.248	0.40	Flag	No Capsize
214	0.092	0.753	0.30	No	No Capsize	323	0.096	1.244	0.10	No	No Capsize
215	0.099	0.755	0.30	No	No Capsize	324	0.100	1.245	0.20	No	No Capsize
216	0.103	0.747	0.40	Flag	Capsize	325	0.100	1.247	0.30	Flag	No Capsize
220	0.094	0.752	0.40	Flag	Capsize	326	0.106	1.254	0.30	No	No Capsize
237	0.068	0.995	0.30	No	No Capsize	327	0.101	1.234	0.40	Flag	Capsize
238	0.069	1.000	0.30	No	No Capsize	329	0.100	1.252	0.40	Flag	No Capsize
239	0.068	0.998	0.40	No	No Capsize	331	0.105	1.228	0.40	Flag	Capsize
240	0.070	1.000	0.40	No	No Capsize	333	0.101	1.254	0.40	Flag	Capsize
276	0.106	0.998	0.20	No	No Capsize	399	0.055	1.486	0.30	No	No Capsize
277	0.102	0.998	0.20	No	No Capsize	400	0.052	1.498	0.40	No	No Capsize
278	0.103	0.993	0.30	No	No Capsize	404	0.069	1.504	0.20	No	No Capsize
280	0.101	0.996	0.40	No	No Capsize	405	0.068	1.496	0.30	No	No Capsize
281	0.102	1.002	0.40	No	No Capsize	406	0.068	1.494	0.40	No	No Capsize
305	0.055	1.250	0.30	No	No Capsize	415	0.100	0.754	0.40	Flag	No Capsize
307	0.052	1.252	0.30	No	No Capsize	417	0.100	0.750	0.40	No	No Capsize
309	0.067	1.242	0.20	No	No Capsize	418	0.097	0.773	0.40	Flag	No Capsize
311	0.070	1.256	0.30	No	No Capsize						

Table 2 shows that runs leading to capsize are consistently flagged by searching for FTLE values in excess of a critical value and/or when behavior is sufficiently anomalous in comparison to other data that insufficient neighbors are found. However, this method also appears overly conservative issuing warnings for non-capsizing runs. Figure 5 gives time histories of roll and $FTLE_1$ for runs which are flagged yet do not lead to capsize. It is apparent that the triggering aspects of the $FTLE_1$ time series occur near very large amplitude motions or even immediately after large motions for cases where roll motion rapidly decreases, as in Run 329, as a particularly striking example. Of primary note

in this figure is that many of these "false positives" occur in runs which are dangerously close to capsize, therefore, providing an operator warning would be prudent for safe operations.

Figure 6 presents the time histories of roll and $FTLE_1$ for those runs leading to capsize, all of which were flagged using this FTLE approach. In Run 327 the flag trigger occurs essentially simultaneously with the catastrophic loss of stability. However, for each of the other four cases, triggers occur prior to capsize, at times even multiple cycles prior to the capsize event.
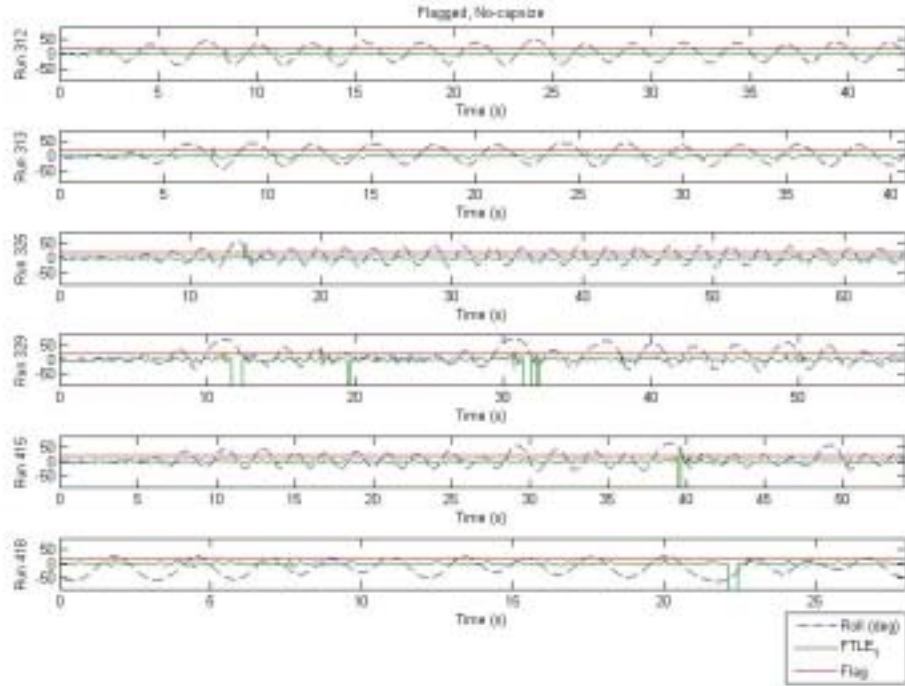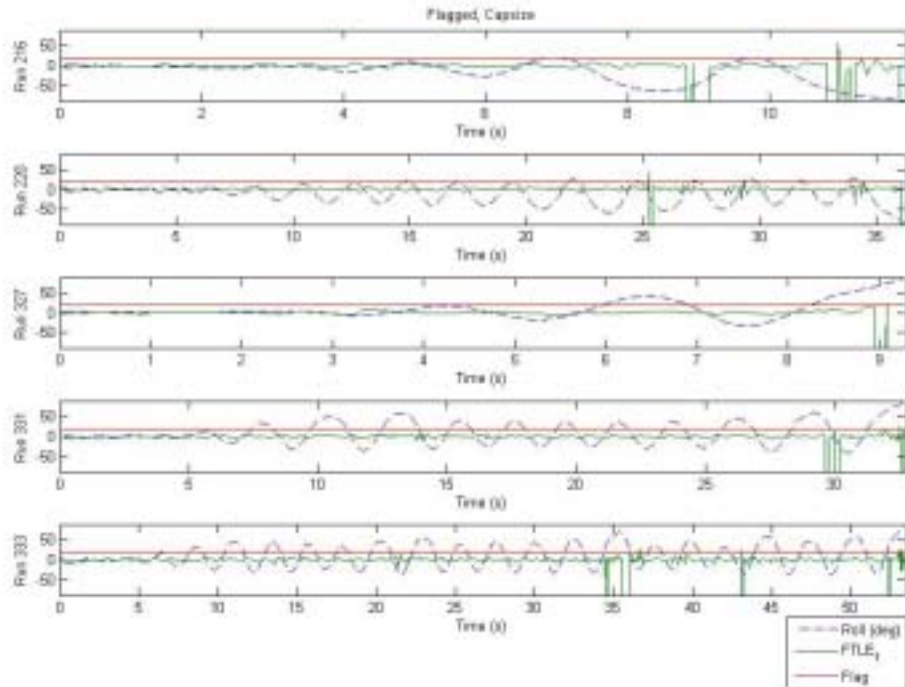
Figure 5: Roll and FTLE1 time series of those runs flagged not leading to capsize. The flag trigger is denoted with a solid horizontal red line, that is, the run is flagged if either the solid green FTLE1 time series exceeds the solid red horizontal line or if there are insufficient neighbors with which to estimate the Jacobian thus causing the FTLE time series to default to a value of -1000, indicated on the figure by those times when FTLE1 exceeds the negative 'y'-ordinate limit of the figure.

Figure 6: Roll and $FTLE_1$ time series of those runs flagged and leading to capsize. The flag trigger is denoted with a solid horizontal red line, that is, the run is flagged if either the solid green $FTLE_1$ time series exceeds the solid red horizontal line or if there are insufficient neighbors with which to estimate the Jacobian thus causing the FTLE time series to default to a value of -1000, indicated on the figure by those times when $FTLE_1$ exceeds the negative 'y'-ordinate limit of the figure.
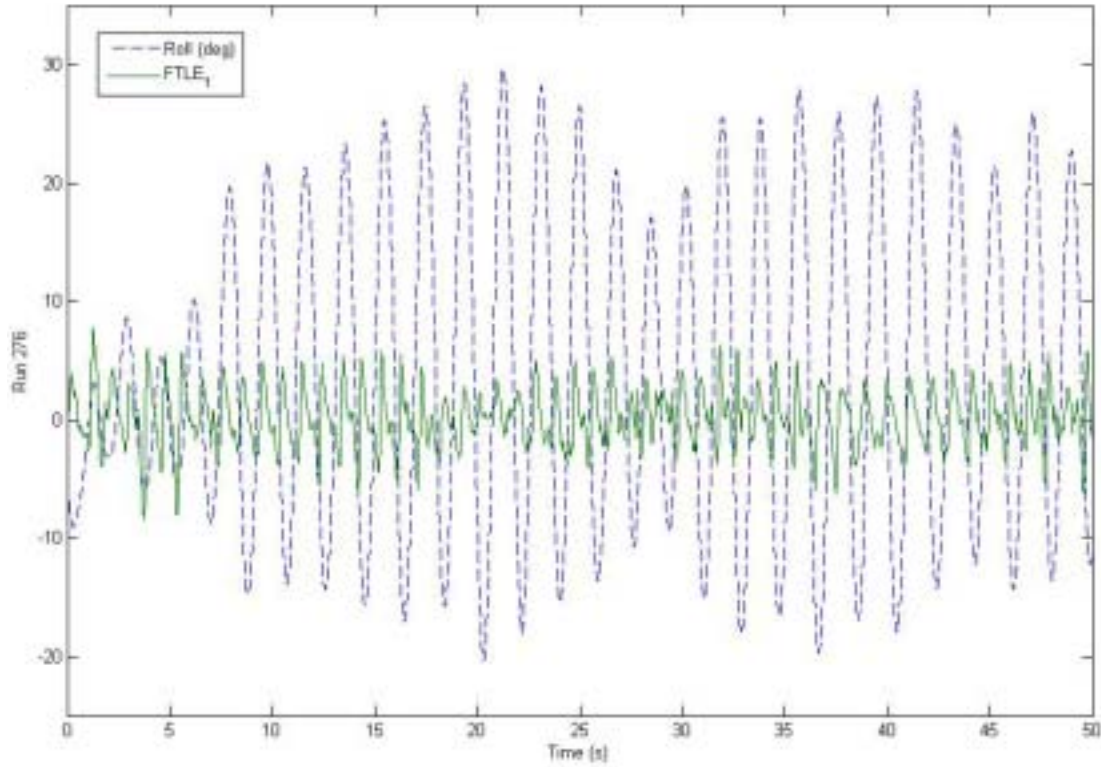
Figure 7: Roll and FTLE$_1$ time series for Run 276

As shown previously (McCue, 2005; McCue & Troesch, 2006; McCue & Bulian, 2006), qualitative changes in the FTLE time series behavior were also noted corresponding to changes in the magnitude of ship motions. For Run 276, a non-capsize, non-flagged case presented in Figure 7, it is apparent that the qualitative behavior, *i.e.* the regularity of the FTLE time series varies as roll motions increase or decrease. Quantifying this qualitative behavior could assist in reducing the number of false warnings and potentially indicate changes to yet more subtle behavior, such as the inverse problem of capsize, that is detecting quiescence for safe at sea launch and recovery operations.

5. CONCLUSIONS

In this work, the authors demonstrate the feasibility of using FTLEs to detect chaotic behavior leading to large amplitude motions and/or capsize as applied to experimental tests conducted in the Maneuvering and Seakeeping Basin at the Carderock Division of the Naval Surface Warfare Center for DTMB Hull 5514. Large fluctuations in the FTLE time series and/or flagging due to insufficient neighbors with which to estimate the Jacobian of the system preceded and coincided with large amplitude motions particularly those leading to capsize.

Future work will include testing this method using simulation-based time histories in random seas. This will allow iteration and optimization of the chosen variables, such as incorporation of yaw. Also, simulated data can provide sufficiently long time histories to allow tests of highly specified scope, *e.g.* limiting the number of conditions included in the search for neighboring points such as only looking at conditions with the same heading and speed and or/conditions with slowly varying heading, speed, and sea states in an effort to emulate realistic operating conditions.

To be useful in an onboard sense the calculation algorithms could easily be modified to search the recent past history of data for the ship as it is operating in any given sea state. As available time series grow longer, *e.g.* if this approach were to be used onboard a ship for some relatively long time period by comparison to the length of the experimental data sets, the accuracy of this method is anticipated to only improve with the precision of the Jacobian estimation. Further study is warranted to quantify qualitative behavior observed in the FTLE time series, identify appropriate bounds for flagging from the FTLE time series, and to ensure warnings are issued in sufficient time for corrective measures so as to enable use of this methodology on-board, in real time as a stand-alone package or as a companion to an intelligent systems or other dynamic motion monitoring approach.

6. ACKNOWLEDGEMENTS

7. REFERENCES

Arnold, L., Chueshov, I., & Ochs, G. 2003. "*Stability and capsizing of ships in random sea-a survey*." Tech. rept. 464. Universität Bremen Institut für Dynamicsche Systeme.

Benettin, G., Galgani, L., Giorgilli, A., & Strelcyn, J.-M. 1980. "Lyapunov characteristic exponents for smooth dynamical systems and for Hamiltonian systems; a method for computing all of them." Meccanica, 9–20.

Eckhardt, B., & Yao, D. 1993. "Local Lyapunov exponents in chaotic systems." *Physica "D*, **65**, 100–108.

Eckmann, J.-P., & Ruelle, D. 1985. "Ergodic theory of chaos and strange attractors." *Reviews of Modern Physics*, **57**(3), 617–656.

Eckmann, J.-P., Oliffson Kamphorst, S., Ruelle, D., & Ciliberto, S. 1986. "Liapunov exponents from time series." *Physical Review A*, **34**(6).

Falzarano, J. M. 1990. "*Predicting complicated dynamics leading to vessel capsizing*." Ph.D. thesis, Department of Naval Architecture and Marine Engineering, University of Michigan, Ann Arbor, MI.

McCue, L. S. 2005 (October). "Applications of finite-time Lyapunov exponents to the study of capsize in beam seas." *In: 8th International Ship Stability Workshop*. Istanbul Technical University, Turkey.

McCue, L. S., & Bassler, C. 2005 (November). "An alternative quiescence detection method for sea-based aviation operations." *In: ASNE's Launch and Recovery of Manned and Unmanned Vehicles from Surface Platforms: Current and Future Trends Symposium*. presentation only.

McCue, L. S., & Bulian, G. 2006 (June). "A numerical feasibility study of a parametric roll advance warning system." *In: 25th International Conference on Offshore Mechanics and Arctic Engineering (OMAE2006)*. ASME, Hamburg, Germany.

McCue, L. S., & Troesch, A. W. 2004 (November). "Use of Lyapunov exponents to predict chaotic vessel motions." *In: 7th International Ship Stability Workshop*. Shanghai Jiao Tong University, China.

McCue, L. S., & Troesch, A. W. 2005 (September). "Identification of nonlinear

and chaotic behavior in model-scale liquefied natural gas (LNG) carrier experimental data." *In: 2005 International Design Engineering Technical Conferences & Computers and Information in Engineering Conference*. ASME, Long Beach, California.

McCue, L. S., & Troesch, A. W. 2006. "A combined numerical-empirical method to calculate finite time Lyapunov exponents from experimental time series with application to vessel capsizing." *Ocean Engineering*. In press.

McCue, L. S., Belknap, W., & Campbell, B. 2005 (October). "Reconciling experimental and numerical data: techniques of nonlinear seakeeping code validation." *In: 8th International Ship Stability Workshop*. Istanbul Technical University, Turkey.

Murashige, S., & Aihara, K. 1998a. "Coexistence of periodic roll motion and chaotic one in a forced flooded ship." *International Journal of Bifurcation and Chaos*, **8**(3), 619–626.

Murashige, S., & Aihara, K. 1998b. "Experimental study on chaotic motion of a flooded ship in waves." *Proceedings of the Royal Society of London A*, **454**, 2537–2553.

Murashige, S., Yamada, T., & Aihara, K. 2000. "Nonlinear analyses of roll motion of a flooded ship in waves." *Philosophical Transactions of the Royal Society of London A*, **358**, 1793–1812.

Papoulias, F. A. 1987. "*Dynamic analysis of mooring systems*." Ph.D. thesis, Department of Naval Architecture and Marine Engineering, University of Michigan, Ann Arbor, MI.

Sano, M., & Sawada, Y. 1985. "Measurement of Lyapunov Spectrum from a Chaotic Time Series." *Physical Review Letters*, **55**(10).

Spyrou, K. J. 1996. "Homoclinic connections and period doublings of a ship advancing in quartering waves." *Chaos*, **6**(2).

Wolf, A., Swift, J., Swinney, H., & Vastano, J. 1985. "Determining Lyapunov exponents from a time series." *Physica D*, **16**, 285–317.